Chemical and Process Engineering Research
ISSN 2224-7467 (Paper) ISSN 2225-0913 (Online)
Vol.27, 2014

Numerical Investigation of the Effects of Reactor Pressure on Biomass Pyrolysis in Thermally Thin Regime

Pious O. Okekunle[1*], Emmanuel A. Osowade[2]

1. Department of Mechanical Engineering, Ladoke Akintola University of Technology, P.M.B. 4000, Ogbomoso, Oyo state, Nigeria.

2. Prototype Engineering Development Institute, Kilometer 4, Eruru Quarters, Ilesa, Osun state, Nigeria.
*Email of the corresponding author: pookekunle@lautech.edu.ng

Abstract

Effects of reactor pressure [vacuum (0.0001, 0.01 atm), atmospheric (1 atm) and pressurized (10, 100 atm) regions] on primary tar production rate, primary tar intra-particle secondary reactions, and tar and gas release rates during pyrolysis in thermally thin regime at a heating rate of 30 K/s and final reactor temperature of 973 K have been numerically investigated. Wood cylinder ($\rho = 400\ kg/m^3$, $\emptyset\ 1\ mm$ and length $1\ mm$) was modeled as a two – dimensional porous solid. Transport equations, chemical kinetic models, pressure and energy conservation equations were coupled and used to simulate the pyrolysis process. Solid mass conservation equations were solved by first-order Euler Implicit Method. Finite volume method was used to discretize the mass conservation equation for argon, primary tar, gas and secondary tar, energy conservation equation and pressure equation. Findings showed that pressure increase, either from vacuum to atmospheric or from atmospheric to pressurized region, has no significant effect on the primary decomposition reactions of the sample. Pressure increase within vacuum region (0.0001 to 0.01 atm) and within pressurized region (10 to 100 atm) has no significant effect on primary tar intra-particle secondary reactions, and tar and gas release rates. However, pressure increase from vacuum to atmospheric and from atmospheric to pressurized region increased primary tar residence time within the pyrolyzing solid thereby enhancing intra-particle secondary reactions.

Keywords: Biomass, pyrolysis, pressure effect, intra-particle secondary reactions, thermally thin regime

1. Introduction

Sustainable energy supply for global development and the need to reduce or alleviate emissions of greenhouse gases have increased interest in seeking alternatives to fossil fuel. Biomass pyrolysis and gasification have been receiving attention for some decades as viable alternative means of energy generation. Temperature, pressure, heating rate and reaction time can influence or determine the proportion and characteristics of the main products of these processes, being thermochemical. Many researchers have investigated the effects of temperature, heating rate and reaction time on biomass pyrolysis [1-10, 14]. Effects of particle shape and size on pyrolysis have also being investigated [11 – 13]. Others have studied the impact of shrinkage, intra-particle heat and mass transfer [15-17]. Aside from the primary decomposition of solid fuels, research works have shown that there are both intra- and extra-particle secondary reactions [18-20]. Effects of biomass size and aspect ratio on intra-particle tar decomposition during pyrolysis have been investigated [21]. Effects of biomass thermo-physical properties on tar intra-particle secondary reactions have also been studied [22]. Findings on the effects of pressure on both primary and secondary reactions during pyrolysis are really scarce. Hajaligol *et al.* [23] had an experimental and modeling study of the effects of pressure on tar release by rapid pyrolysis of cellulose sheets in a screen heater. They concluded that at 1000 $^oC/s$ heating rate, tar secondary reactions are significant within the fuel piece at pressures near and above 1 atm, and temperatures greater than or equal to the range 650-750 ^oC, and external to the fuel piece, including on the heater screen, at 0.0001 atm and greater than or equal to 800 ^oC. They further observed that pressures other than atmospheric can occur in scientifically and practically important situations where cellulosic solids undergo rapid pyrolysis, for example, combustion or gasification of wood and other biomass, burning of solid propellants, detonation of solid explosives, and thermal degradation of materials. Despite this, very few works have been

reported in this aspect. As a result, this study was aimed at numerically investigating the effects of reactor pressure on biomass pyrolysis in thermally thin regime with emphasis on primary tar production and intra-particle secondary reactions.

2. Pyrolysis Mechanism

Several mechanisms have been used to explain various phenomena taking place during biomass pyrolysis [23]. Figure 1 shows the structure of the mechanism used in this study. Detailed explanation on the development of this mechanism has been reported in our earlier research works [21,24]. As shown in Figure 1, wood first decomposes by three endothermic competing primary reactions to form gas, primary tar and intermediate solid. The primary tar undergoes secondary reactions to yield secondary tar, more gas and char. The intermediate solid also undergoes secondary reaction to yield only char. Reaction rates were assumed to follow Arrhenius expression of the form: $k_i = A_i \exp\left(-E_i/RT\right)$. The chemical kinetic ($A$ and E) and thermodynamic (a and b) parameters are as given in one of our previous works [24].

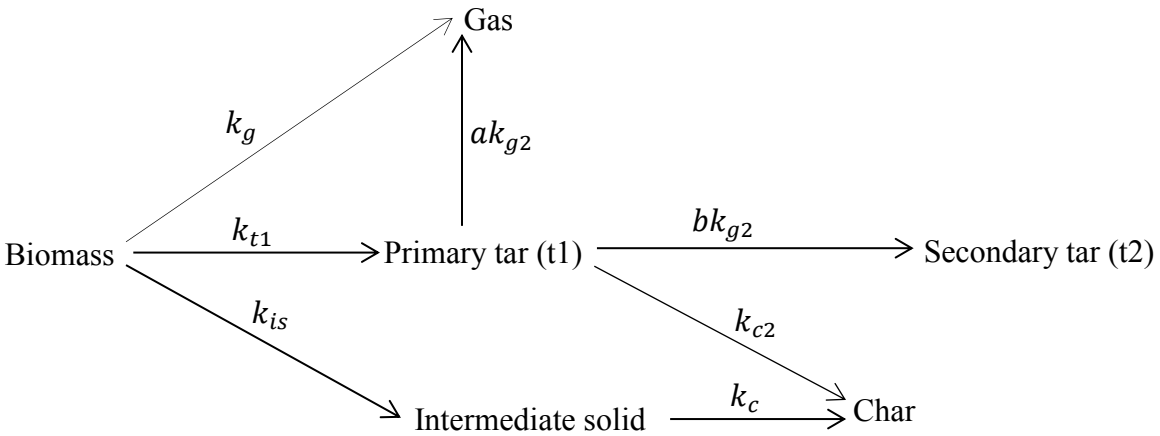

Figure 1: Schematic illustration of the pyrolysis mechanism

3. Numerical Simulation

Because the governing equations, model assumptions and numerical procedures in this study are the same as in the previous studies [21, 22, 24], a brief account is given here.

3.1 Solid mass conservation equation

The instantaneous mass balance of the pyrolyzing solid comprises three endothermic consumption terms yielding gas, tar and intermediate solid:

$$\frac{\partial \rho_s}{\partial t} = -(k_g + k_t + k_{is})\rho_s \quad (1)$$

The intermediate solid instantaneous mass balance equation (equation (2)) contains two terms, one for the conversion of the virgin solid to intermediate solid and the other from exothermic decomposition of intermediate solid to yield char, given as

$$\frac{\partial \rho_{is}}{\partial t} = k_{is}\rho_s - k_c\rho_{is} \quad (2)$$

In the same vein, the char instantaneous mass balance equation (equation (3)) contains two terms, one from the exothermic decomposition of intermediate solid and the other from primary tar secondary reaction to yield char, given as

$$\frac{\partial \rho_c}{\partial t} = k_c \rho_{is} + k_{c2} \rho_t \quad (3)$$

3.2 Mass conservation equations of gas phase components

Mass conservation equations for all gas phase components are expressed by two-dimensional cylindrical coordinate system consisting of both temporal and spatial gradients and source terms

$$\text{Ar: } \frac{\partial(\varepsilon \rho_{Ar})}{\partial t} + \frac{\partial(\rho_{Ar} U)}{\partial z} + \frac{1}{r}\frac{\partial(r \rho_{Ar} V)}{\partial r} = S_{Ar}, \quad (4)$$

$$\text{Gas: } \frac{\partial(\varepsilon \rho_g)}{\partial t} + \frac{\partial(\rho_g U)}{\partial z} + \frac{1}{r}\frac{\partial(r \rho_g V)}{\partial r} = S_g, \quad (5)$$

$$\text{Primary tar : } \frac{\partial(\varepsilon \rho_{t1})}{\partial t} + \frac{\partial(\rho_{t1} U)}{\partial z} + \frac{1}{r}\frac{\partial(r \rho_{t1} V)}{\partial r} = S_{t1}, \quad (6)$$

$$\text{Secondary tar: } \frac{\partial(\varepsilon \rho_{t2})}{\partial t} + \frac{\partial(\rho_{t2} U)}{\partial z} + \frac{1}{r}\frac{\partial(r \rho_{t2} V)}{\partial r} = S_{t2} \quad (7)$$

S_{Ar} , S_g, S_{t1} and S_{t2} are the source terms for the carrier gas (argon), gas, primary tar and secondary tar, respectively, and are given by

$$S_{Ar} = 0 \quad (8)$$

$$S_g = k_g \rho_s + \varepsilon k_{g2} \rho_{t1} \quad (9)$$

$$S_{t1} = k_t \rho_s - \varepsilon [k_{c2} + (a+b) k_{g2}] \rho_{t1} \quad (10)$$

$$S_{t2} = \varepsilon b k_{g2} \rho_{t1} \quad (11)$$

Intra-particle tar and gas transport velocity was estimated by Darcy's law,

$$U = -\frac{B}{\mu}\left(\frac{\partial P}{\partial z}\right) \quad (12)$$

$$V = -\frac{B}{\mu}\left(\frac{\partial P}{\partial r}\right) \quad (13)$$

where B and μ are respectively the charring biomass solid permeability and kinematic viscosity. Porosity,ε, is expressed as

$$\varepsilon = 1 - \frac{\rho_{s,sum}}{\rho_{w,0}} (1 - \varepsilon_{w,0}) \quad (14)$$

where $\varepsilon_{w,0}, \rho_{s,sum}$ and $\rho_{w,0}$ are the initial porosity of the wood, the sum of solid mass density and initial wood density, respectively. The permeability, B, of the charring biomass is expressed as a linear interpolation between the solid phase components, given as

$$B = (1 - \eta) B_w + \eta B_c \quad (15)$$

where η is the degree of pyrolysis and is defined as

$$\eta = 1 - \frac{\rho_s + \rho_{is}}{\rho_{w,0}} \quad (16)$$

3.3 Energy conservation equation

The energy conservation equation is given as

$$\left(C_{p,w}\rho_s + C_{p,w}\rho_{is} + C_{p,c}\rho_c + \varepsilon C_{p,t}\rho_{t1} + \varepsilon C_{p,t}\rho_{t2} + \varepsilon C_{p,g}\rho_g\right)\frac{\partial T}{\partial t} = \frac{\partial}{\partial z}\left(k_{eff(z)}\frac{\partial T}{\partial z}\right) + \frac{1}{r}\frac{\partial}{\partial r}\left(rk_{eff(r)}\frac{\partial T}{\partial r}\right) - l_c\Delta h_c - \sum_{i=g,t1,is} m_i\Delta h_i - \varepsilon\sum_{i=g2,t2,c2} n_i\Delta h_i \quad (17)$$

where

$$l_c = A_c \exp(-E_c/RT)\,\rho_{is} \quad (18)$$

$$m_i = A_i \exp(-E_i/RT)\,\rho_s \quad i = g, t1, is \quad (19)$$

$$n_i = A_i \exp(-E_i/RT)\,\rho_{t1} \quad i = g2, t2, c2 \quad (20)$$

Effective thermal conductivity of the particle consists of both the conductive and radiative terms and is expressed as

$$k_{eff(i)} = k_{cond(i)} + k_{rad} \qquad (i = z, r) \quad (21)$$

where k_{cond} is estimated as the weighted sum of the thermal conductivities of the virgin wood, char and volatiles, and varies with the degree of virgin wood conversion. It is given by

$$k_{cond(i)} = (1-\eta)k_{w(i)} + \eta k_{c(i)} + \varepsilon k_v \qquad (i = z, r) \quad (22)$$

The radiative thermal conductivity through the pores is given by

$$k_{rad} = \frac{13.5\sigma T^3 d_{pore}}{e} \quad (23)$$

where σ, e and d_{pore} are Stefan-Boltzmann constant, emissivity and pore diameter, respectively. Table 1 presents the thermo-physical properties of the wood sample.

3.4 Pressure evolution

The total pressure is the sum of the partial pressures of the inert gas (argon), gas and secondary tar from the pyrolysis process. It is given as

$$P = P_{Ar} + P_{t2} + P_g;\;\; P_i = \frac{\rho_i RT}{M_i} \qquad (i = Ar, t2, g) \quad (24)$$

where M_i and R are the molecular weight of each gaseous species and universal gas constant, respectively. Combining equations (4), (5), (7), (12), (13) and (24), intra-particle pressure equation was obtained as

$$\frac{\partial}{\partial t}\left(\varepsilon\frac{P}{T}\right) - \frac{\partial}{\partial r}\left[\frac{BP}{\mu T}\left(\frac{\partial P}{\partial z}\right)\right] - \frac{1}{r}\frac{\partial}{\partial r}\left[r\frac{BP}{\mu T}\left(\frac{\partial P}{\partial r}\right)\right] = \frac{R}{M_{t2}}S_{t2} + \frac{R}{M_g}S_g \quad (25)$$

3.5 Numerical Procedure

Wood cylinder was modeled as a two-dimensional isotropic porous solid. Wood pores were assumed to be initially filled with argon. As the solid was pyrolyzed, tar and gas were formed while argon was displaced to the outer region without participating in the pyrolysis reaction. The solid mass conservation equations (eqs (1) – (3)) were solved by first-order Euler Implicit Method. The mass conservation equations for argon, primary tar, gas and secondary tar (eqs (4) – (7)), energy conservation equation (eq. (17)) and the pressure equation (eq. (25)) were discretized using finite volume method. Hybrid differencing scheme was adopted for the convective terms. First-order fully implicit

scheme was used for the time integral with time step of 0.005 s. The detailed numerical procedure and calculation domain have been given somewhere else [24]. Model assumptions have also been given the previous work [22].

Table 1: Thermo-physical properties of the wood sample

Property	Value	Reference
$C_{p,w}$	$1500 + 1.0T$ [J/kg K]	[25]
$C_{p,c}$	$420 + 2.0T + 6.85 \times 10^{-4}T^2$ [J/kg K]	[25]
$C_{p,t}$	$-100 + 4.4T + 1.57 \times 10^{-3}T^2$ [J/kg K]	[25]
$C_{p,g}$	$770 + 0.629T - 1.91 \times 10^{-4}T^2$ [J/kg K]	[25]
d_{pore}	$5 \times 10^{-5}(1-\eta) + 1 \times 10^{-4}\eta$ [m]	[25]
σ	5.67×10^{-8} [W/m^{2}K^4]	[25]
B_w	5×10^{-16} [m^2]	[25]
B_c	1×10^{-13} [m^2]	[25]
e	0.95 [−]	[26]
h_c	8.4×10^{-3} [W/m^2 K^{-1}]	[2]
μ	3.0×10^{-5} [kg/m s]	[25]
$k_{w(r)}$	0.1046 [W/m K]	[25]
$k_{w(z)}$	0.2550 [W/m K]	[25]
$k_{c(r)}$	0.0710 [W/m K]	[25]
$k_{c(z)}$	0.1050 [W/m K]	
k_v	0.0258 [W/m K]	[25]
$\varepsilon_{w,o}$	0.4 [−]	[25]
M_g	0.038 [kg/mol]	[25]
M_{t1}	0.162 [kg/mol] (assumed to be levoglucosan)	
M_{t2}	0.11 [kg/mol]	
R	8.314 [J/mol K]	[25]

4. Results and discussion

4.1 Effect of pressure on weight loss

Figure 2 (a) –(c) shows the weight loss history of the biomass material at different reactor pressures (0.0001, 1 and 100 atm, representing vacuum, atmospheric and pressurized regions, respectively). When reactor pressure is 0.0001 atm (Fig. 2a), active disintegration of biomass sample began at 6 s elapsed time and continued until about 13 s. After 13 s, weight loss appeared insignificant. Weight loss profile is similar for all reactor pressures considered. This implies that a change in reactor pressure during biomass pyrolysis does not affect primary tar production reaction of the feedstock.

4.2 Primary tar production rate

Figure 3 shows primary tar production rate at different reactor pressures. From the figure, primary tar production rate profiles are uniform in all cases. As shown in the pyrolysis mechanism (Figure 1), primary tar production reaction is one of the three parallel and competing initial reactions undergone by the biomass sample. This result suggests further that changes in reactor pressure have no significant effect on the primary pyrolysis of woody biomass in thermally thin regime.

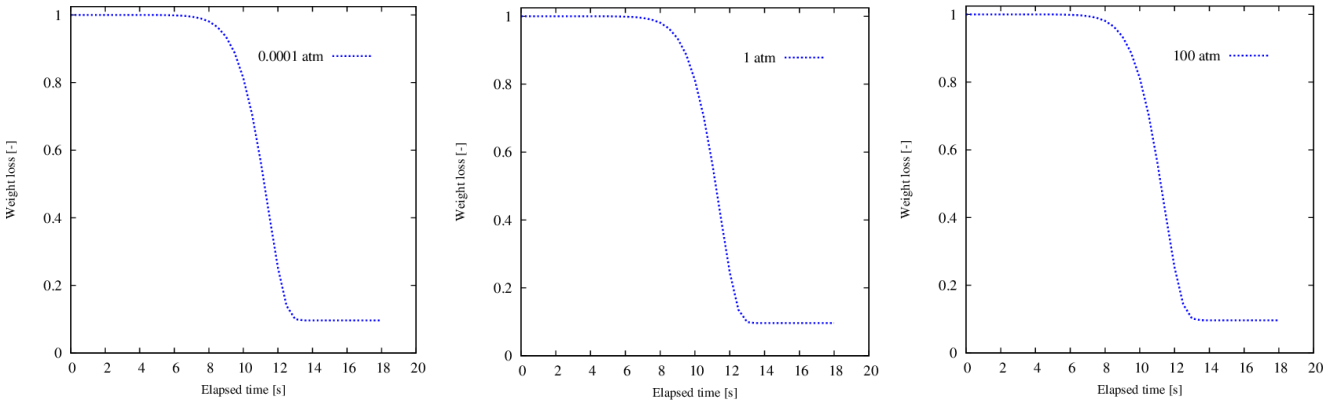

(a) (b) (c)

Figure 2: Weight loss history at different reactor pressures

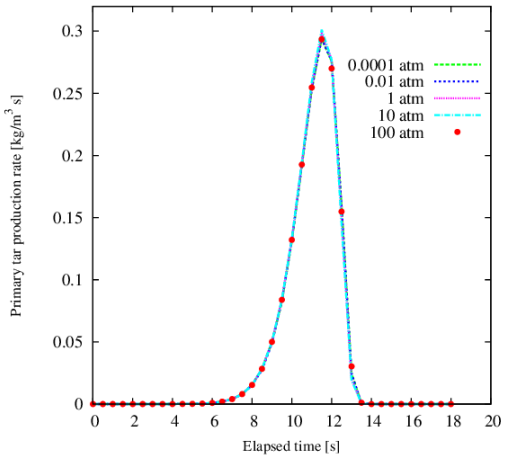

Figure 3: Rate of primary tar production at different reactor pressure

4.3 Primary tar secondary reactions

For quantitative analysis of intra-particle secondary reactions at different reactor pressures, the rate of products generation during these reactions was estimated. Figure 4 shows the rate of products generation from primary tar secondary reactions at different reactor pressures. From the figure, increase in pressure within the vacuum region did not have any significant effect on products generation rate. However, as pressure increased from vacuum to atmospheric, products generation rate from primary tar secondary reactions was significantly increased, getting to its peak at about 12.3 s. Pressure increase from atmospheric to 10 atm further increased the rate of products generation from intra-particle secondary reactions. Pressure increase beyond 10 atm has no noticeable effect on the rate of products generation from tar intra-particle secondary reactions. This implies that as the reactor pressure increases from vacuum to atmospheric region, and from atmospheric to pressurized region, tar transport within the pyrolyzing

solid is inhibited, thereby making more time available for consumption of primary tar through intra-particle secondary reactions with attendant increase in gas mixture mass flux.

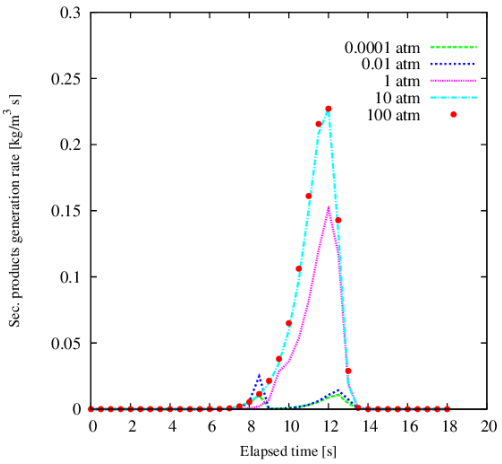

Figure 4: Rate of products generation from primary tar secondary reactions at different reactor pressures

4.4 Gas release rate

Figure 5 shows the mass flux of gas mixture at different reactor pressure. From the figure, below atmospheric pressure i.e. vacuum (0.0001 and 0.01 atm), the mass flux of gas mixture was not affected by increase in reactor pressure (from 0.0001 to 0.01 atm). As reactor pressure increased from vacuum to atmospheric however, there was a sharp increase in gas mass flux from the pyrolyzing solid. As the reactor pressure was increased from atmospheric to 10 atm, there was a further increase in gas mixture mass flux. Further increase in reactor pressure from 10 atm to 100 atm had no effect on gas mixture mass flux. The pressure variation ranges can be subdivided into three regions: vacuum (pressure < 1 atm), atmospheric (pressure = 1 atm) and pressurized (pressure > 1 atm). This result can be explained by considering tar transport and tar secondary reactions. As reactor pressure increased from vacuum region to atmospheric, tar transport from the surface of the pyrolyzing solid was inhibited, thereby giving more time for tar intra-particle secondary reactions, which may be both homogeneous (within the pores of pyrolyzing solid) and heterogeneous (over fresh wood char surfaces). Only homogeneous secondary reactions are however considered in this study. Since the main product of tar secondary reactions is gas, mass flux of gas mixture was therefore increased. This fact also explains the phenomenon of increase in gas mixture mass flux from atmospheric to pressurized region. This result is in agreement with the findings of Hajaligol *et al.* [23].

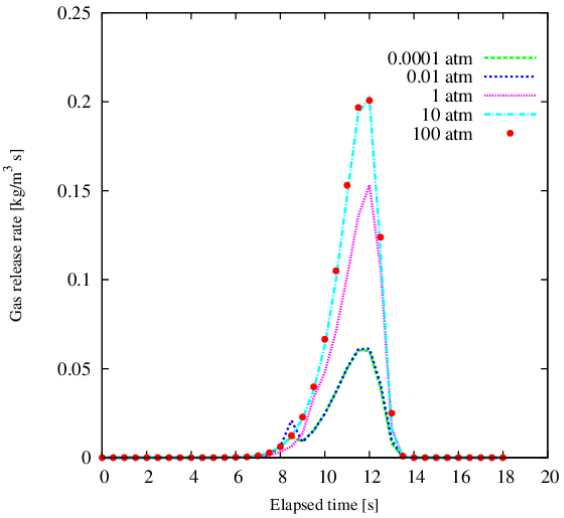

Figure 5: Gas release rate at different reactor pressures

4.5 Tar release rate

Figure 6 shows tar release rate from the pyrolyzing solid at different reactor pressures. From the figure, the rate of tar release is highest in the vacuum region (where reactor pressure is less than 1 atm). At this region, increase in pressure did not have any effect on the rate of tar release (i.e. tar yield is not strongly sensitive to pressure increase in this region). As the reactor pressure increased from vacuum to atmospheric, there was a significant reduction in the rate of tar release, the reason being that more molecules of tar generated from primary pyrolysis have been consumed in intra-particle secondary reactions to yield secondary tar, more gas and char. As the reactor pressure increased above atmospheric, there was a further decrease in the rate of tar release from the pyrolyzing solid. This was due to the fact that a higher percentage of tar produced from primary pyrolysis was consumed in intra-particle secondary reactions. This implies that tar transport within the pyrolyzing solid was further inhibited as the reactor pressure increased above atmospheric. In the pressurized region (region above atmospheric condition), further increase in pressure does not have any significant effect on tar release rate.

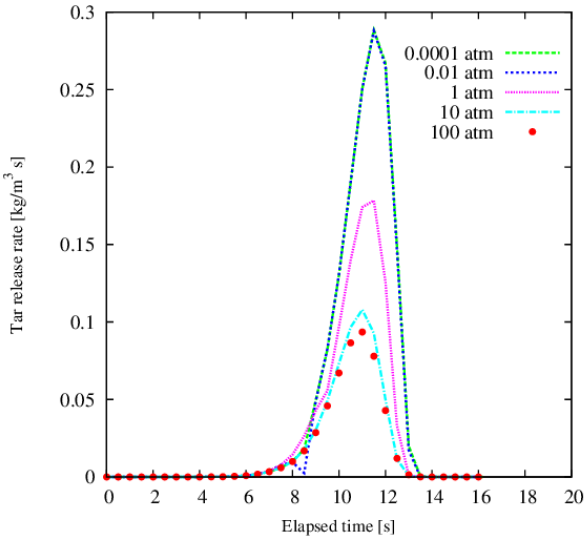

Figure 6: Tar release rate at different reactor pressure

5. Conclusions

From this study, it is understood that reactor pressure (inert gas pressure) can strongly influence product yield distribution, and tar and gas release rates during pyrolysis of biomass in thermally thin regime. For pyrolysis of woody biomass, at 30 K/s and final reactor temperature of 973 K, it can be concluded that in vacuum region, homogenous tar intra-particle secondary reactions are not significantly influenced by pressure increase. Therefore within this region, any change in product yield distribution, and tar and gas release rates due to increase in reactor pressure will be caused mainly by heterogeneous intra-particle tar secondary reactions and extra-particle secondary reactions. In atmospheric and pressurized regions, however, homogeneous intra-particle tar secondary reactions are significantly influenced by change in pressure. Therefore, change in product yield distribution, and tar and gas release rates, as reactor pressure increases from vacuum to atmospheric, will be largely influenced by homogeneous intra-particle tar secondary reactions. This scenario also holds as reactor pressure increases from atmospheric to pressurized region. However, further reactor pressure increase within pressurized region (where $P > 1$ atm) will not have any significant effect on homogeneous tar intra-particle reactions. Any changes in product yield distribution, and the rates of tar and gas release in this case will be largely dependent on heterogeneous intra-particle tar secondary reactions and extra-particle secondary reactions.

Nomenclature

A: pre-exponential factor	(1/s)
B: permeability	(m^2)
Cp: specific heat capacity	(J/ kg K)
E: activation energy	(J/mol)
e: emissivity	(-)
h_c: convective heat transfer coefficient	(W/ m^2 K)
k: reaction rate constant	(1/s)
k_c: char thermal conductivity	(W/m K)
k_w: wood thermal conductivity	(W/m K)
M: molecular weight	(kg/mol)
P: Pressure	(Pa)
Q: heat generation	(W/m^3)
Q_c: convective heat flux	(W/m^2)
Q_r: radiation heat flux	(W/m^2)
R: universal gas constant	(J/mol K)
R: total radial length	(m)
r: radial direction	
z: axial direction	
S: source term	
T: temperature	(K)
t : time	(s)
U: axial velocity component	(m/s)
V: radial velocity component	(m/s)
ε: porosity	(-)
ε_0: initial porosity	(-)
Δh: heat of reaction	(kJ/kg)
μ: viscosity	(kg/m s)
ρ: density	(kg/m^3)
ρ_{w0}: initial density of wood	(kg/m^3)
σ: Stefan-Boltzmann constant	(W/m^2 K^4)
η: degree of pyrolysis	

Subscripts
Ar: Argon
c: char, primary char formation reaction

c_2: secondary char formation reaction
g: gas, primary gas formation reaction
g_2: secondary gas formation reaction
is: intermediate solid, intermediate solid formation reaction
s: solid
t: tar, tar formation reaction
v: total volatile
w: wood

References

[1] Scotts, D.S., Piskorz, J., Bergougnou, M.A., Graham, R. & Overend, R.P. (1988). The Role of Temperature in the Fast Pyrolysis of Cellulose and Wood. *Industrial Chemistry Research* **27**, 8-15.
[2] Pyle, D.L.& Zaror, C.A. (1984). Heat Transfer and Kinetics in the Low Temperature Pyrolysis of Solid. *Chemical Engineering Science* **19**, 147-158.
[3] Piskorz, J., Majerski, P., Radlein, D., Scott, D.S. and Bridgwater, A.V. (1998). Fast Pyrolysis of Sweet Sorghum and Sweet Sorghum Bagasse. *Journal of Analytical and Applied Pyrolysis* **46**, 15-29.
[4] Horne, P.A. & Williams, P.T. (1996). Influence of Temperature on the Products from the Flash Pyrolysis of Biomass. *Fuel* **75**, 1051-1059.
[5] Antal, M.J. (1983). Effects of Reactor Severity on the Gas-phase Pyrolysis of cellulose and Kraft Lignin-derived Volatile Matter. *Industrial Engineering Production Research and Development* **22**, 366-375.
[6] Scott, D.S. & Piskorz, J. (1982). The Flash Pyrolysis of Aspen-poplar Wood. *Canadian Journal of Chemical Engineering* **60**, 666-674. In Modeling Chemical and Physical processes of Wood and Biomass Pyrolysis, Progress in Energy and Combustion Science, 34 (2008), 47-90.
[7] Di Blasi, C., Branca, C., Santoro, A. & Gonzalec Hernandez, E. (2001). Pyrolytic Behaviour and Products of Some Wood Varieties. *Combustion and Flame* **124**, 165-177
[8] Di Blasi, C. and Branca, C. (2001). Kinetics of primary Product Formation from Wood Pyrolysis. *Industrial Engineering Chemistry Research* **40**, 5547-5556.
[9] Miller, R.S. and Bellan, J. (1997). A Generalized Biomass Pyrolysis Model Based on Superimposed Cellulose, Hemicellulose and Lignin Kinetics, *Combustion Science and Technology* **126**, 97-137.
[10] Miller, R.S. and Bellan, J. (1996). Analysis of Reaction Products and Conversion Time in the Pyrolysis of cellulose and Wood Particles. *Combustion Science and Technology* **119**, 331-373.
[11] Lu, H., Ip, E., Scott, J., Foster, P., Vickers, M. and Baxter, L.L. (2010). Effects of Particle Shape and Size on Devolatilization of Biomass particle. *Fuel* **89**, 1156-1168.
[12] Chan, W.R., Kelbon, M. and Krieger, B.B. (1985). Modelling and Experimental Verification of Physical and Chemical Processes during Pyrolysis of a Large Biomass Particle. *Fuel* **64**, 1505-1513.
[13] Liliedahl, T. and Sjöström, K. (1998). Heat Transfer Controlled Pyrolysis Kinetics of a Biomass Slab, Rod or Sphere. *Biomass and Bioenergy* **15(6)**, 503-509.
[14] Fushimi, C., Araki, K., Yamaguchi, Y. and Tsutsumi, A. (2003). Effect of Heating Rate on Steam Gasification of Biomass. 2. Thermogravimetric-Mass Spectrometic (TG-MS) Analysis of Gas Evolution. *Industrial Engineering Chemistry Research* **42**, 3929-3936.
[15] Papadikis, K., Gu, S. and Bridgwater, A.V. (2009). CFD Modelling of the Fast Pyrolysis of Biomass in Fluidized Bed Reactors. Modeling the Impact of Biomass Shrinkage. *Chemical Engineering Journal* **149**, 417-427.
[16] Bharadwaj, A., Baxter, L.L. and Robinson A.L. (2004). Effects of Intraparticle Heat and Mass Transfer on Biomass Devolatilization: Experimental Results and Model Predictions. *Energy & Fuel* **18**, 1021-1031.
[17] Hagge M.J. and Bryden, K.M. (2002). Modeling the Impact of Shrinkage on the Pyrolysis of Dry Biomass. *Chemical Engineering Science* **57**, 2811-2823.
[18] Boroson, M.L., Howard, J.B., Longwell, J.P. and Peters, W.A. (1989). Heterogeneous Cracking of Wood pyrolysis Tars Over Fresh Wood Char Surfaces. *Energy& Fuels* **3**, 735-740.
[19] Fraga, A., Gaines, A.F. and Kandiyoti, R. (1991). Characterization of Biomass Pyrolysis Tars Produced in the Relative Absence of Extraparticle Secondary Reactions. *Fuel* **70**, 803-809.
[20] Gilot, P. and Stanmore, B.R. (1995). A Theoretical Study of the Mechanism of Intraparticle Mass Transport of Volatiles During Pyrolysis of Nonsoftening Coal. Application to Secondary Tar Reactions. *Energy & Fuels* **9**,

126-135.
[21] Okekunle, P.O., Watanabe, H., Pattanotai, T. & Okazaki, K. (2012). Effect of Biomass Size and Aspect Ratio on Intra-particle Tar Decomposition during Wood Cylinder Pyrolysis. *Journal of Thermal Science and Technology*, **7(1)**, 1-15.
[22] Okekunle, P.O. (2013). Numerical Investigation of the Effects of Thermo-physical Properties on Tar Intra-particle Secondary Reactions during biomass Pyrolysis. *Mathematical Theory and Modeling* **3(14)**, 83-97.
[23] Di Blasi, C. (2008) Modeling Chemical and Physical Processes of Wood and Biomass Pyrolysis. *Progress in Energy and Combustion Science* **34**, 47-90.
[24] Okekunle, P.O., Pattanotai, T., Watanabe, H. and Okazaki, K. (2011). Numerical and Experimental Investigation of Intra-particle Heat Transfer and Tar Decomposition during Pyrolysis of Wood Biomass. *Journal of Thermal Science and Technology* **6(3)**, 360-375.
[25] Park, W.C., Atreya, A. and Baum, H.R. (2010). Experimental and Theoretical Investigation of Heat and Mass Transfer during Wood Pyrolysis. *Combustion and Flame* **157**, 481-494.
[26] Babu, B.V. and Chaurasia, A.S. (2003). Modeling for Pyrolysis of Solid particle: Kinetics and Heat Transfer Effects. *Energy Conversion and Management* **44**, 2251-2275.

The IISTE is a pioneer in the Open-Access hosting service and academic event management. The aim of the firm is Accelerating Global Knowledge Sharing.

More information about the firm can be found on the homepage:
http://www.iiste.org

CALL FOR JOURNAL PAPERS

There are more than 30 peer-reviewed academic journals hosted under the hosting platform.

Prospective authors of journals can find the submission instruction on the following page: http://www.iiste.org/journals/ All the journals articles are available online to the readers all over the world without financial, legal, or technical barriers other than those inseparable from gaining access to the internet itself. Paper version of the journals is also available upon request of readers and authors.

MORE RESOURCES

Book publication information: http://www.iiste.org/book/

IISTE Knowledge Sharing Partners

EBSCO, Index Copernicus, Ulrich's Periodicals Directory, JournalTOCS, PKP Open Archives Harvester, Bielefeld Academic Search Engine, Elektronische Zeitschriftenbibliothek EZB, Open J-Gate, OCLC WorldCat, Universe Digtial Library , NewJour, Google Scholar